Phase Equilibrium Measurements of Methane + Benzene and Methane + Methylbenzene at Temperatures from (188 to 348) K and Pressures to 13 MPa

Thomas J. Hughes,[a] Mohamed E. Kandil,[a] Brendan F. Graham,[a] Kenneth N. Marsh,[a] Stanley H. Huang,[b] and Eric F. May[a,*]

[a] Centre for Energy, School of Mechanical & Chemical Engineering, University of Western Australia, Crawley, WA, Australia 6009
[b] Chevron Energy Technology Company, Houston TX 77002, U.S.A.

Abstract

New isothermal *pTxy* data are reported for methane + benzene and methane + methylbenzene (toluene) at pressures up to 13 MPa over the temperature range (188 to 313) K using a custom-built vapor-liquid equilibrium (VLE) apparatus. The aim of this work was to investigate literature data inconsistencies and to extend the measurements to lower temperatures. For methane (1) + benzene (2), measurements were made along six isotherms from (233 to 348) K at pressures to 9.6 MPa. At temperatures below 279 K there was evidence of a solid phase, and thus only vapor phase samples were analyzed at these temperatures. For the methane (1) + methylbenzene (3) system, measurements were made along seven isotherms from (188 to 313) K at pressures up to 13 MPa. Along the 198 K isotherms, a significant change in the data's p,x slope was observed indicating liquid-liquid equilibria at higher pressures. The data were compared with literature data and with calculations made using the Peng-Robinson (PR) equation of state (EOS). For both binary systems our data agree with much of the literature data that also deviate from the EOS in a similar manner. However, the data of Elbishlawi and Spencer (*Ind. Eng. Chem.* **1951**, *43*, 1811-1815) for both binary systems, which appear to have received an equal weighting to other data in the EOS development, are inconsistent with the results of our measurements and data from other literature sources.

Keywords: methane, benzene, methylbenzene, toluene, vapor liquid equilibria, equations of state.

* Corresponding Author. E-mail: Eric.May@uwa.edu.au, Tel +61 8 6488 2954

Introduction

Accurate vapor-liquid equilibrium (VLE) data for hydrocarbon systems are required for many reasons including the development of improved equations of state, which are used in a variety of upstream and downstream hydrocarbon transport and processing applications. There are numerous VLE data sets in the literature for binary hydrocarbon systems but many of the measurements are inconsistent with each other. In this work we present new measurements of VLE for the methane (1) + benzene (2) and methane (1) + methylbenzene (3) systems to help resolve such inconsistencies in the literature data. In addition, we present results indicative of a liquid-liquid equilibrium (LLE) for the methane + methylbenzene system at 198.15 K, a higher temperature than has been reported or was expected [1]. The phase equilibria of these particular systems are important for multiple reasons: for example, in natural gas processing the solubility of methane in these aromatic compounds is important in estimating the methane content of the bottoms product of demethanizer distillation column. Aromatic components in natural gas have also been shown to be a concern in low pressure natural gas pipelines made from plastics, as the pipelines are vulnerable to solvation if the aromatics condense [2].

Our previous papers described the construction of a cryogenic VLE apparatus for measurements at high pressure, and measurements were made on the systems methane + 2-methylpropane [3], methane + pentane and methane + hexane [4]. These data were compared with calculated values from the multi-parameter GERG-2008 EOS for natural gases [5] using mole fraction deviation plots. However, the GERG-2008 EOS has not been extended to include aromatic compounds, which precludes comparisons similar to those given previously [3; 4]. Therefore in this work the deviation plots have been prepared using the PR EOS as implemented in the "PR (Advanced)" model set in the software Infochem Multiflash [6] as the baseline. This EOS is referred to as advanced [7] because the temperature dependence of the equation's "*a*" parameter is optimized to replicate experimental vapor pressure data, and a Peneloux volume translation correction [8] is also implemented. For both mixtures in this work the default symmetric temperature independent BIPs were used in calculations (k_{12} = 0.0301, k_{13} = 0.0334). Significant differences between the literature measurements and our data were observed, including differences of 0.05 or larger in the liquid phase

methane mole fractions. Additionally, our measurements of the methane + methylbenzene system at a temperature of 198.15 K exhibited what Lin et al [1] referred to as a "reverse solubility" trend at high pressures, which indicates LLE rather than VLE. This temperature is somewhat higher than the upper value for LLE of 192 K estimated by Lin et al [1], although the PR EOS used in this work also predicted LLE at 198.15 K.

Method and Materials

The suppliers and supplier-analyzed purities of all components used in this work are listed in Table 1. Our analysis of these compounds by gas chromatography indicated no detectable impurities.

The experimental apparatus and technique have been described in detail previously [3; 4; 9]; the improvements described by Kandil et al. [4] for the methane + hexane measurements were implemented in this work. For methane + benzene, measurements were made along six isotherms from (233 to 348) K, at pressures from (2.1 to 9.6) MPa. The cell was first evacuated and flushed several times with pure methane then, while filled with methane at $p \approx 0.2$ MPa, approximately 10 mL of liquid benzene was pumped into the cell using a high pressure liquid chromatograph (HPLC) pump. To ensure the benzene in the cell was degassed, the system was kept at 290 K and the valve to the vacuum pump was momentarily opened, with the stirrer on. After 2 h of intermittent evacuation it was assumed that the liquid was completely degassed. The cell was then held at the desired temperature while methane gas was added to achieve the target pressure. The sample was mixed and once it had reached equilibrium, up to five samples from both the gas and liquid phases were removed and analyzed with a gas chromatograph (GC). The next measurement at a different pressure, on the same isotherm, was made by either adding methane or venting the vapor phase. The isotherm sequence was as follows: starting at 323 K the temperature was increased to the highest temperature of 348 K, then decreased to 278 K, followed by a measurement at 268 K and then at 233 K. Measurements at 278 K were then repeated followed by measurements at 303 K. Finally, a single measurement was made at 323 K and about 8 MPa. At 268 K and 233 K, the time series pressure results indicated the existence of a

solid phase (see the Results and Discussion section), which is consistent with the known triple point temperature of pure benzene (T_t = 278.67 K) [10].

For the methane + methylbenzene system, measurements were made along seven isotherms from (188 to 313) K, at pressures from (1.9 to 13.2) MPa. The method of loading and changing the pressure in the cell was the same as described for the methane + benzene system. In particular the amount of methane added was not measured precisely; it was simply added until the specific target pressure was achieved. Along the T = 198.15 K isotherm a change in slope of the p,x data was observed, indicating the presence of a LLE at higher pressures.

To enable quantitative VLE measurements with a rigorous uncertainty assessment, the two flame ionization detectors (FID) of the gas chromatograph were calibrated, following on a method similar to that described in our previous work [4], to determine the response factor ratios (κ_i/κ_1) of the FIDs for the three compounds methane (i = 1), benzene (i = 2), methylbenzene (i = 3). The detector response factors κ_i are defined in eq 1 of Kandil et al [4], and a summary of the results of the calibration is listed in Table 2, where FID-L and FID-V are the flame ionisation detectors for the nominal liquid and vapor phases, respectively. These ratios were used to determine the values of x_1, y_2, and y_3 listed in Tables 2 and 3.

To determine (κ_2/κ_1), three binary liquid mixtures of benzene (2) + hexane (4) with x_2 ≈ 0.18, 0.52 and 0.85 were injected through the GC's liquid sampling manifold. Unfortunately, the liquid sampling manifold used to inject the gravimetrically prepared liquid calibration mixtures onto the GC could only be connected to FID-L, and thus it was assumed that (κ_2/κ_4) and (κ_3/κ_4) were the same for both detectors. In the future, a switch to allow a sample to be sent to either detector will be added to the GC; however such a test was not possible at the time of these measurements. The ratio (κ_2/κ_4) was measured to be 1.040 ± 0.002 and multiplied by the ratio (κ_4/κ_1) determined in Kandil et al [4] (5.57 ± 0.13 for FID-L and 5.61 ± 0.21 for FID-V) to obtain the ratio (κ_2/κ_1) = 5.80 ± 0.13 for FID-L and 5.84 ± 0.21 for FID-V. The same procedure was followed to determine the ratio (κ_3/κ_1) by injecting three binary liquid mixtures of methylbenzene (3) + hexane (4) with x_3 ≈ 0.28, 0.5 and 0.77 through the GC's liquid sampling manifold.

The ratio (κ_3/κ_1) was then similarly determined by multiplying the ratio (κ_3/κ_4) measured to be 1.134 ± 0.003 by the ratio (κ_4/κ_1) determined in Kandil et al [4] as above, to obtain the ratio (κ_3/κ_1) = 6.32 ± 0.13 for FID-L and 6.36 ± 0.21 for FID-V. These values of (κ_2/κ_1) and (κ_3/κ_1) had relative uncertainties of about 3 % and were consistent with those estimated from the detector response factors tabulated by Dietz [11], as 5.62 and 6.33 who also reported a relative uncertainty of about 3 %.

Uncertainties: The estimated uncertainties of the measurements for methane (1) + benzene (2) are listed in Table 3, and for methane (1) + methylbenzene (3) in Table 4. The temperatures listed in Tables 2 and 3 are the average of the bottom and lid thermometers of the cell. The composition uncertainties were obtained by combining in quadrature the uncertainties arising from the temperature gradient along the cell, the standard deviation of the temperature over the course of the measurement, and the uncertainty of the calibration of the platinum resistance thermometers give a value of $u(T) \approx 0.10$ K.

For pressure, the standard uncertainty was $0.005 \cdot p$ in the range from (1 to 14) MPa, provided the temperature was within the range from (150 to 333) K. The pressure uncertainty was calculated from the quadrature combination of the standard deviation of the Kulite transducer's calibration with the standard deviation of the pressure reading during the measurement. It had a maximum value of $u(p) \approx 0.05$ MPa for the methane + benzene at the maximum pressure of 10.7 MPa, and $u(p) \approx 0.07$ MPa for the methane + methylbenzene at the maximum pressure of 13.2 MPa.

The uncertainties in the composition measurements for the liquid phase $u(x_1)$ and for the vapor phase $u(y_i)$, listed in Tables 2 and 3, are the quadrature combination of the standard deviation in measurements (calculated from the five repeat measurements at each pressure and temperature), the uncertainty of the ratio of the FID response coefficients (κ_i/κ_1) listed in Table 2 and the effects of propagating the temperature and pressure uncertainties (these contributions were assessed by investigating the change in the compositions by perturbing $T \pm u(T)$ and $p \pm u(p)$ using the PR EOS). In Kandil et al. [4] the relative composition uncertainties $u(x_1)/x_1$ and $u(y_i)/y_i$ were both about 0.04 for methane + pentane and methane + hexane systems, although as expected at low

hexane vapor fractions ($y_i < 0.002$), $u(y_i)/y_i$ increased rapidly to a maximum of 1.5. In this work the relative uncertainties for methane + benzene and methane + methylbenzene were larger with $u(x_1)/x_1$ w0.1 and $u(y_i)/y_i \approx 0.1$, although for $y_i < 0.005$ $u(y_i)/y_i$ increased to a maximum of 3 for methylbenzene. Furthermore, $u(x_1)/x_1$ for the methane + methylbenzene system exhibited significantly more scatter than observed previously [3; 4] or for the methane + benzene system. This increase in the relative uncertainty of the liquid methane mole fraction can be attributed to two effects: the decrease in (sampling) repeatability at low temperatures and high pressures (for the methane + methylbenzene system), and the lower range of x_1 observed for these aromatic liquids. In this work the ranges ($0.037 \le x_1 \le 0.172$) for methane + benzene, and ($0.046 \le x_1 \le 0.28$) for methane + methylbenzene were significantly smaller than in our previous work [4] for which ($0.11 \le x_1 \le 0.96$), and hence the relative uncertainties in x_1 increased accordingly.

Results and Discussion

Comparison with Literature Data:† The measurements for methane (1) + benzene (2) are listed in Table 3. There appears to be no literature data reported for methane (1) + benzene (2) at T = 233.15 K and 268.15 K and, in this work, only vapor phase compositions were measured at these temperatures. There was evidence of solid formation at temperatures below 273 K, as shown in Figure 1, which is consistent with the known triple point temperature of pure benzene (T = 278.67 K) [10]. It was also consistent with the predictions of solid-vapor equilibrium (SVE) at these conditions made using Multiflash's solid freeze-out model [7] with the PR (advanced) model set. Thus, only the vapor phase was sampled at 233.15 K and 268.15 K.

In Figure 2, the measured p,x data for methane (1) + benzene (2) are plotted. In Figure 3a the deviations (x_1 - $x_{1,calc}$) of the measured methane liquid mole fraction, x_1, from those calculated with the PR EOS at the same pressure and temperature, $x_{1,calc}$, are plotted. In addition to our measurements, data from the literature are also plotted [2; 12; 13; 14; 15; 16; 17; 18; 19; 20; 21]. Only the data of Elbishlawi and Spencer [14],

† Graphical p,x comparisons of our measurements with the available literature data along several isotherms for both systems are shown in the supplementary material.

Stepanova et al. [21], Rijkers et al. [19] and Darwish et al. [13] are within the x_1, p and T range of our measurements. However, the data of Luks et al. [17] were only just outside the temperature range (our lowest temperature was 278.15 K and their highest temperature was 277.7 K) and the data of Sage et al. [20] were measured at only slightly higher mole fractions (our highest x_1 was 0.172 and their lowest x_1 was 0.1799). Our data appear to be in reasonable agreement with the literature data of Stepanova et al. [21], Luks et al. [17], and Rijkers et al. [19]. The data of Sage et al. [20], Elbishlawi and Spencer [14] and Darwish et al. [13] are inconsistent with our results, as they have increased methane mole fractions in the liquid phase. In particular, the data of Elbishlawi and Spencer [14] deviate from equivalent data measured in this work and elsewhere by methane liquid mole fractions as large as (0.03 to 0.04). The purity of methane used by Elbishlawi and Spencer [14] was low ("not less than" than a mole fraction of 0.99 methane), containing mole fractions of 0.005 ethane and 0.003 nitrogen as well as "traces of carbon dioxide" [14] Additionally, Elbishlawi and Spencer [14] estimated the composition of the liquid and vapor phases from measurements of their gas densities using a Dumas bulb, a method which we note is susceptible to large uncertainties [22].

In Figure 3a there are also some large deviations between the literature measurements and PR EOS predictions, up to and exceeding a mole fraction of 0.15. The literature data sets in general agree on the trend with deviations from the EOS switching from negative to postive as both x_1 and T increase. There is a fair amount of scatter in the literature data over the whole composition range but as our measurements do not go beyond $x_1 = 0.172$ they can not be used to identify between which of the data in this region are likely more accurate. More high quality data are needed at higher liquid mole fractions of methane to confirm which data are reliable, as there are some large discrepancies. For example at $x_1 \approx 0.43$ and $T = 293$ K for the methane (1) + benzene (2) system there is about a 0.046 mole fraction discrepancy between the data of Rijkers et al [19] and the Stepanova et al [21] despite, as we note above, that their results appear relatively consistent with our data at lower mole fractions of methane. Without corroborated data for much of the mole fraction range efforts to optimize equation of state predictions for this mixture would likely be premature.

In Figure 3b the deviations (y_1 - $y_{1,calc}$) of the measured methane vapor mole fraction, y_1, from those calculated with the PR EOS at the same pressure and temperature, $y_{1,calc}$, are plotted together with the corresponding deviations calculated for literature data. The data of Elbishlawi and Spencer [14], Stepanova et al. [21], Coan and King [12], Legret et al [15], Rijjkers et al. [2] and Marteau et al. [18] were measured in the same range of y_1, p and T as our measurements. Our data are in reasonable agreement with most of these data though we note that the data of Elbishlawi and Spencer [14] and Legret et al. [15] tend to deviate postively from our data. From both deviation plots presented in Figure 3a and 2b we conclude that the data of Elbishlawi and Spencer [14] are likely erroneous given their significant postive deviations from our data and other literature data.

For methane (1) + methylbenzene (3), our VLE measurements are listed in Table 4 and LLE measurements are listed in Table 5. Liquid-liquid equilibrium measurements were reported by Lin et al. [1] at 189 K, who observed a change in the slope of their p,x data. Chang and Kobayashi [23] had previously observed LLE visually in the system methane + methylbenzene at low temperatures. However, based on measurements made about a decade later, Lin et al. (also from the Kobayashi group at Rice University) subsequently concluded that the data of Chang and Kobayashi [23] were erroneous.

In Figure 4 our VLE data are plotted on a p,x diagram. In Figure 5a the deviations (x_1 - $x_{1,calc}$) of the measured methane liquid mole fraction, x_1, from those calculated using the PR EOS at the same pressure and tempearture, $x_{1,calc}$, are plotted for our measurements along with deviations calculated for the literature data. Only the data of Lin et al. [1] are within the T range of our measurements. At 228 K, the deviations of our data are slightly more negative than those of Lin et al.'s data at 233 K (by about $\Delta x_1 \approx 0.02$) but at higher temperatures ($T > 250$ K) our data are up to 0.045 mole fraction below those of Lin et al. Unfortunately there are no other data sources in this temperature range, which would be particularly useful for $x_1 > 0.28$ where the data of Lin et al. indicate an unusual temperature dependence: as shown in Figure 5a, their mole fraction deviations at 255 K are initially more positive than the deviations at 277 K and then the two sets cross-over at about $x_1 \approx 0.46$ and a mole fraction deviation of -0.089. Such anomalous behavior should be investigated further and more high quality measurements at $x_1 >$

0.28 are clearly needed. The data of Elbishlawi and Spencer [14] deviate significantly in a positive manner from all other data sets measured at similar temperatures, as was the case for the methane + benzene system.

In Figure 5b the deviations (y_1 - $y_{1,calc}$) of the measured methane vapor mole fraction, y_1, from those calculated with the PR EOS at the same pressure and temperature, $y_{1,calc}$, are plotted together with the corresponding deviations for the literature data. The data of Hwang and Kobayashi [24], Lin et al. [1], Legret et al. [15], and Schlichting et al. [25] are within the T range of our measurements and deviate from the EOS predictions by less than a mole fraction of 0.007.

For both binary systems, the VLE data of Elbishlawi and Spencer [14] appear to be inconsistent with all of the available measurements at corresponding conditions. Yet the deviations of their data from the EOS suggest that they have been given a weighting equal to or greater than those of other measurements during the model's development. The results of this work indicate that in any future EOS development for these binary systems, the data of Elbishlawi and Spencer [14] should be excluded.

Figure 6 shows LLE phase diagrams for methane (1) + methylbenzene (3). In Figure 6a our data and the data of Lin et al. [1] are plotted along with the full extent of the calculated LLE and VLE phase boundaries using the PR EOS (as implemented in the PR (advanced) model set in Multiflash). In Figure 6b a close-up of the bubble point and methylbenzene-rich LLE lines is shown. Comparison of our data at 198.15 K with the corresponding PR EOS predictions shows a significant difference between the experimental vapor-liquid-liquid equilibrium (VLLE) point at approximately x_1= 0.205 and p = 5.0 MPa and the calculated point at x_1= 0.362 and p = 5.8 MPa. However, the experimental and calculated slopes for the methylbenzene-rich LLE line to the right of this point in the (p,x_1) plane are both positive and similar in magnitude. In contrast the slope of the LLE line measured by Lin et al at T = 188.71 K was negative while the calculated slope at this temperature was positive. As at 198.15 K, there is a significant difference between the VLLE point at 188.71 K measured by Lin et al at x_1 = 0.2652 and p = 4.34 MPa and predicted with the equation of state at x_1 = 0.369 and p = 4.33 MPa.

In Figure 6c a close-up of the dew point and methane-rich LLE line are shown. Our measured mole fractions show small deviations (Δx_1 = 0.001 or less) from those calculated by the EOS. The measured mole fractions of Lin et al. for their (V)LLE data points however, deviate from those calculated by the EOS by about a factor of ten greater than the deviations of the measurements reported here. More high quality LLE measurements for this system are needed to investigate these discrepancies and allow the PR EOS or another EOS to be optimized for calculations of LLE.

Conclusions

Three main conclusions can be drawn from this work. First our data at 198.15 K for the methane (1) + methylbenzene (3) system indicate that LLE exists for this system at temperatures higher than expected based on the results of previous measurements [1]. Interestingly, however, LLE at this temperature was predicted using the Peng Robinson EOS. Second, the data of Elbishlawi and Spencer [14] for both methane + benzene and methane + methylbenzene have been shown to be inconsistent with data measured at similar p and T and we recommend that they are not used in the development of equations of state. It appears that these erroneous data were weighted highly in previous model development processes. Finally, it is apparent that high quality literature data are needed at $x_1 > 0.3$ for both methane (1) + benzene (2) and methane (1) + methylbenzene (3) to investigate discrepancies in the available data. Once these discrepancies are resolved equations of state could be optimized with greater confidence.

Acknowledgements

The research was funded by Chevron Energy Technology Company, the Western Australian Energy Research Alliance and the Australian Research Council. The authors thank Craig Grimm for helping to construct and maintain the apparatus. We also thank Jerry Guo and Sean McCallum for their assistance with the measurements. The authors are also grateful to Jeff Buckles for his contributions to the project. We thank the manuscript referees for their valuable comments and suggestions.

Supplementary material

Graphical p,x comparisons of our measurements with the available literature data along several isotherms for both systems are presented. Reasons for any discrepancies are hypothesised.

TABLES

Table 1. Material purities and suppliers

Material	Supplier	Supplier Mole Fraction Purity	Supplier Analysis Method
methane	Air Liquide	0.99995	GC[a,b,c]
benzene	Sigma-Aldrich	0.9991	GC[a,c]
methylbenzene	Sigma-Aldrich	0.9998	GC[a,c]

[a] Gas chromatography

[b] Reported mole fraction impurities from the suppliers analysis were less than $25 \cdot 10^{-6}$ air, $15 \cdot 10^{-6}$ C_2H_6, $5 \cdot 10^{-6}$ H_2O, $5 \cdot 10^{-6}$ other hydrocarbons and $1 \cdot 10^{-6}$ CO_2.

[c] Reported mole fraction impurity of water was less than 0.0001

Table 2. Calibration results for the GC's flame ionisation detectors. The angled brackets denote an average over all measurements. The calibrations for methane and hexane were reported in Kandil et al. [4] Liquid solutions of benzene + hexane and methylbenzene + hexane could only be injected into the manifold for FID-L.

	methane (1)	benzene (2)	methylbenzene (3)	hexane (4)
		FID-L		
Min(A_i) / (10^6 counts)	0.03	4.176	7.033	0.12
Max(A_i) / (10^6 counts)	157.90	24.24	19.517	19.69
$\langle\kappa_i\rangle$ / (10^{13} counts/mol)	3.65	20.91	22.03	19.98
$u(\langle\kappa_i\rangle)$ / (10^{13} counts/mol)	0.20	0.21	1.44	1.45
κ_i / κ_1	1	5.80	6.32	5.57
$u(\kappa_i / \kappa_1)$		0.13	0.13	0.13
		FID-V		
Min(A_i) / (10^6 counts)	0.04			0.11
Max(A_i) / (10^6 counts)	70.80			4.24
$\langle\kappa_i\rangle$ / (10^{13} counts/mol)	3.59			20.05
$u(\langle\kappa_i\rangle)$ / (10^{13} counts/mol)	0.21			1.71
κ_i / κ_1		5.84	6.36	5.61
$u(\kappa_i / \kappa_1)$		0.21	0.21	0.21

Table 3. Measured Phase Compositions for Methane (1) + Benzene (2).[a]

T[a] / K	p / MPa	$u(p)$ / MPa	x_1	$u(x_1)$[b]	y_2	$u(y_2)$[b]	Predicted Equilibrium [d]
348.15	2.337	0.012	0.037	0.005	0.0494	0.0005	VLE
348.15	4.496	0.022	0.079	0.006	0.0341	0.0006	VLE
348.15	6.691	0.034	0.119	0.007	0.0325	0.0005	VLE
348.15	9.615	0.048	0.165	0.006	0.0386	0.0005	VLE
323.15	2.176	0.011	0.040	0.005	0.0298	0.0005	VLE
323.15	3.540	0.018	0.063	0.005	0.0229	0.0005	VLE
323.15	5.171	0.026	0.091	0.006	0.0202	0.0006	VLE
323.15	8.075	0.040	0.141	0.005	0.0220	0.0008	VLE
303.15	2.213	0.011	0.041	0.005	0.0129	0.0005	VLE
303.15	5.535	0.028	0.100	0.007	0.0095	0.0006	VLE
303.15	8.573	0.043	0.151	0.007	0.0113	0.0006	VLE
278.15	2.294	0.011	0.046	0.005	0.0105	0.0009	VLE
278.15	4.485	0.028	0.089	0.006	0.0101	0.0006	VLE
278.15	5.774	0.029	0.104	0.006	0.0079	0.0019	VLE
278.15	5.801	0.029	0.106	0.006	[c]	[c]	VLE
278.15	7.634	0.038	0.140	0.006	0.0067	0.0005	VLE
278.15	7.640	0.039	0.139	0.007	0.0078	0.0017	VLE
278.15	7.824	0.039	0.145	0.005	0.0042	0.0005	VLE
268.15	2.087	0.010			0.0025	0.0005	SVE
268.15	3.572	0.018			0.0022	0.0005	SVE
268.15	6.294	0.031			0.0038	0.0006	SVE
233.15	2.096	0.011			0.0007	0.0005	SVE
233.15	3.597	0.018			0.0008	0.0005	SVE
233.15	6.470	0.033			0.0010	0.0005	SVE
233.15	8.228	0.041			0.0006	0.0005	SVE

[a] $u(T) = 0.10$ K

[b] $u(x_1)$ and $u(y_2)$ include the effect of the propagated temperature and pressure uncertainties on the measured compositions combined with the uncertainties of the composition measurements.

[c] The vapor phase samples acquired at (278.15 K, 5.801 MPa) did not give repeatable values of y_2 and hence were omitted.

[d] The predicted phase equilibrium type from Multiflash's PR (advanced) model set [6].

Table 4. Measured Vapor-Liquid Equilibrium Phase Compositions for Methane (1) + Methylbenzene (3)

T[a] / K	p / MPa	$u(p)$ / MPa	x_1	$u(x_1)$[b]	y_3	$u(y_3)$[b]
313.15	2.686	0.014	0.055	0.005	0.0105	0.0008
313.15	4.114	0.021	0.084	0.005	0.0078	0.0008
293.15	3.264	0.019	0.073	0.009	0.0036	0.0009
293.15	3.933	0.020	0.087	0.009	0.0058	0.0009
293.15	4.773	0.030	0.106	0.005	0.0032	0.0008
293.15	7.567	0.040	0.162	0.006	0.0036	0.0008
293.15	10.418	0.056	0.209	0.009	0.0075	0.0010
277.65	2.923	0.015	0.070	0.005	[c]	[c]
277.65	4.011	0.020	0.091	0.005	[c]	[c]
277.65	6.019	0.031	0.134	0.005	0.0038	0.0009
277.65	8.093	0.041	0.173	0.005	0.0031	0.0008
277.65	13.192	0.066	0.257	0.006	0.0050	0.0009
253.15	1.907	0.010	0.053	0.005	0.0076	0.0008
253.15	2.977	0.015	0.078	0.005	0.0047	0.0009
253.15	4.208	0.021	0.108	0.005	0.0018	0.0008
253.15	6.078	0.030	0.145	0.007	0.0016	0.0008
228.15	2.367	0.012	0.083	0.006	0.0018	0.0009
228.15	3.982	0.020	0.127	0.006	0.0011	0.0008
228.15	5.386	0.048	0.162	0.006	0.0019	0.0008
228.15	7.222	0.036	0.196	0.015	0.0033	0.0009
228.15	8.791	0.044	0.226	0.006	0.0021	0.0010
228.15	10.444	0.052	0.253	0.018	0.0017	0.0008
228.15	13.215	0.066	0.279	0.010	0.0038	0.0008
198.15	1.986	0.010	0.092	0.025	[c]	[c]
198.15	4.337	0.022	0.181	0.016	0.0003	0.0008
188.15	2.353	0.014	0.138	0.021	0.0003	0.0008
188.15	3.368	0.017	0.202	0.038	0.0003	0.0008

[a] $u(T) = 0.10$ K

[b] $u(x_1)$ and $u(y_3)$ include the effect of the propagated temperature and pressure uncertainties on the measured compositions combined with the uncertainties of the composition measurements.

[c] The vapor phase samples acquired at these conditions did not give repeatable values of y_3 and hence are omitted.

Table 5. Measured Liquid-Liquid Equilibrium Phase Compositions for Methane (1) + Methylbenzene (3). The methane-rich liquid is denoted by the superscript L1 and the methylbenzene rich liquid is denoted by the superscript L3.

T[a]	p	$u(p)$	x_1^{L3}	$u(x_1^{L3})$[b]	x_3^{L1}	$u(x_3^{L1})$[b]
K	MPa	MPa				
198.15	8.256	0.041	0.227	0.009	0.0016	0.0008
198.15	6.374	0.032	0.217	0.025	0.0007	0.0008
198.15	8.295	0.044	0.226	0.008	0.0014	0.001
198.15	11.015	0.056	0.251	0.013	0.0043	0.0008
198.15	11.531	0.066	0.244	0.005	0.0036	0.0008

[a] $u(T) = 0.10$ K

[b] $u(x_1^{L3})$ and $u(x_3^{L1})$ include the effect of the propagated temperature and pressure uncertainties on the measured compositions combined with the uncertainties of the composition measurements.

[c] The methane rich liquid samples acquired at these conditions did not give repeatable values of y_3 and hence are omitted.

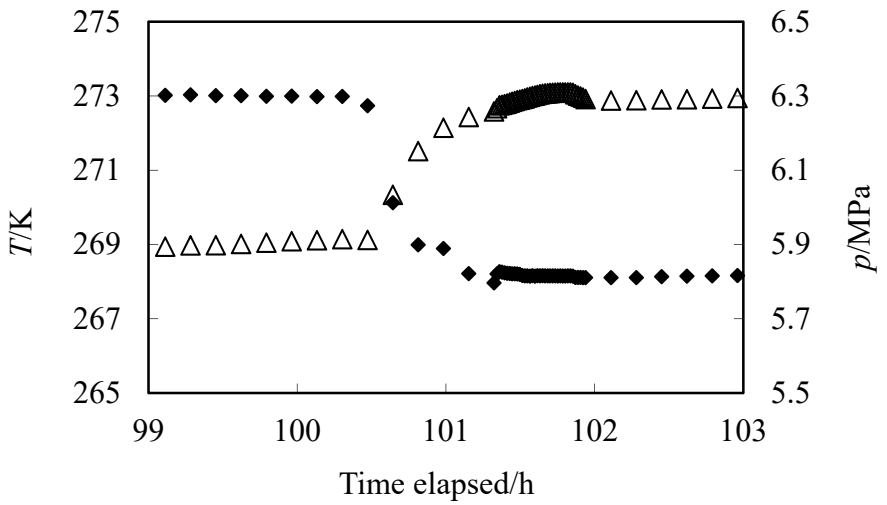

Figure 1. Time series data for the measured temperature and pressure after decreasing the temperature below 273 K. The resulted increase in pressure can be evidence of a solid formation at temperatures below this point. The pressure increased, plausibly, due to expelling the dissolved methane from the solid phase to the vapor phase after the freezing out of benzene from the liquid phase, ◆, *T*; Δ, *p*.

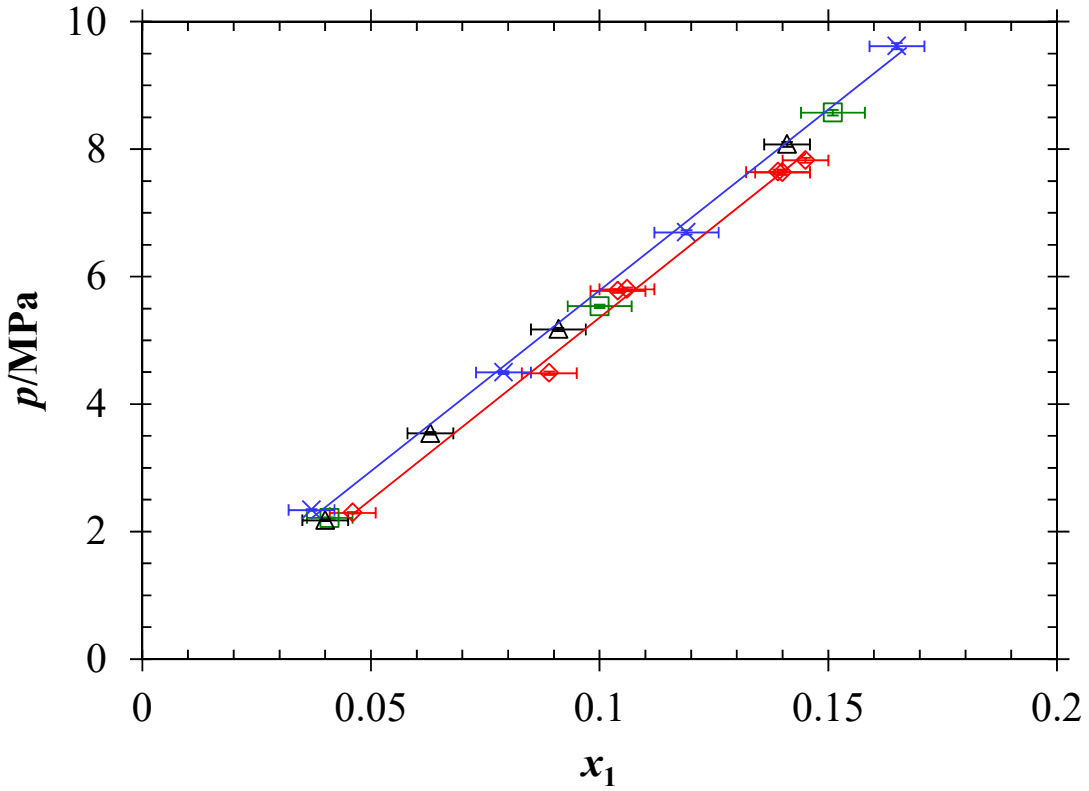

Figure 2. Measured vapor-liquid equilibrium *p, x* data for the methane (1) + benzene (2): ◊, $T = 278.15$ K; □, $T = 303$ K; Δ, $T = 323.15$ K; ×, $T = 348.15$ K. Linear trendlines are shown to guide the eye for the $T = 278.15$ K and $T = 348.15$ K isotherms.

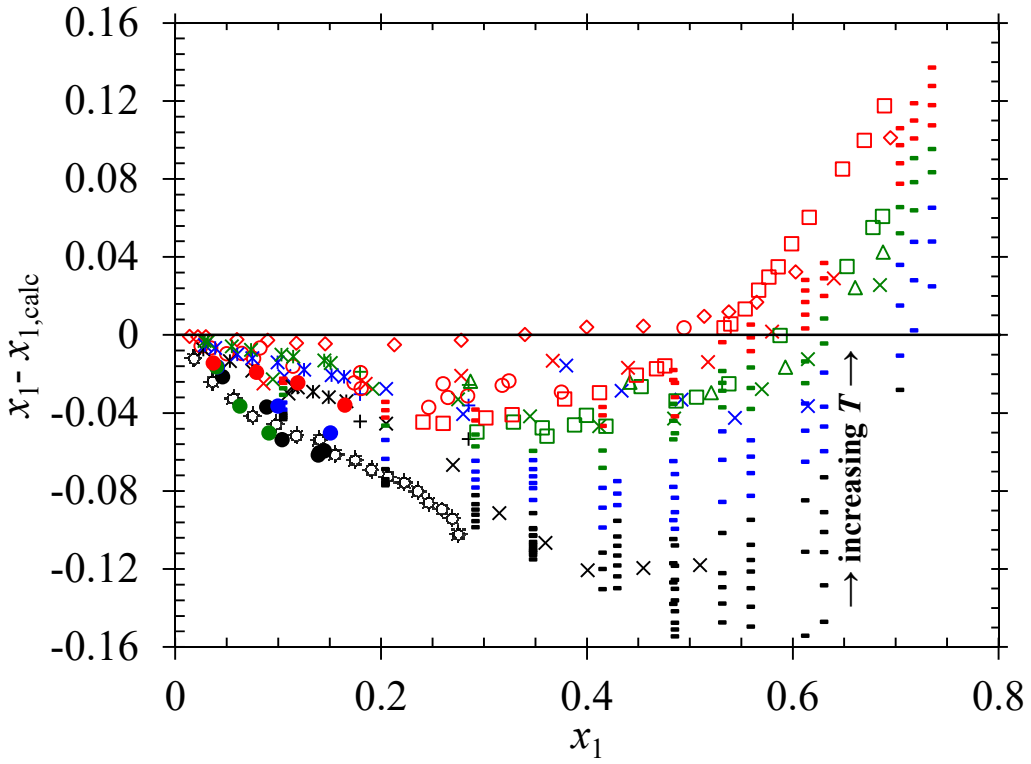

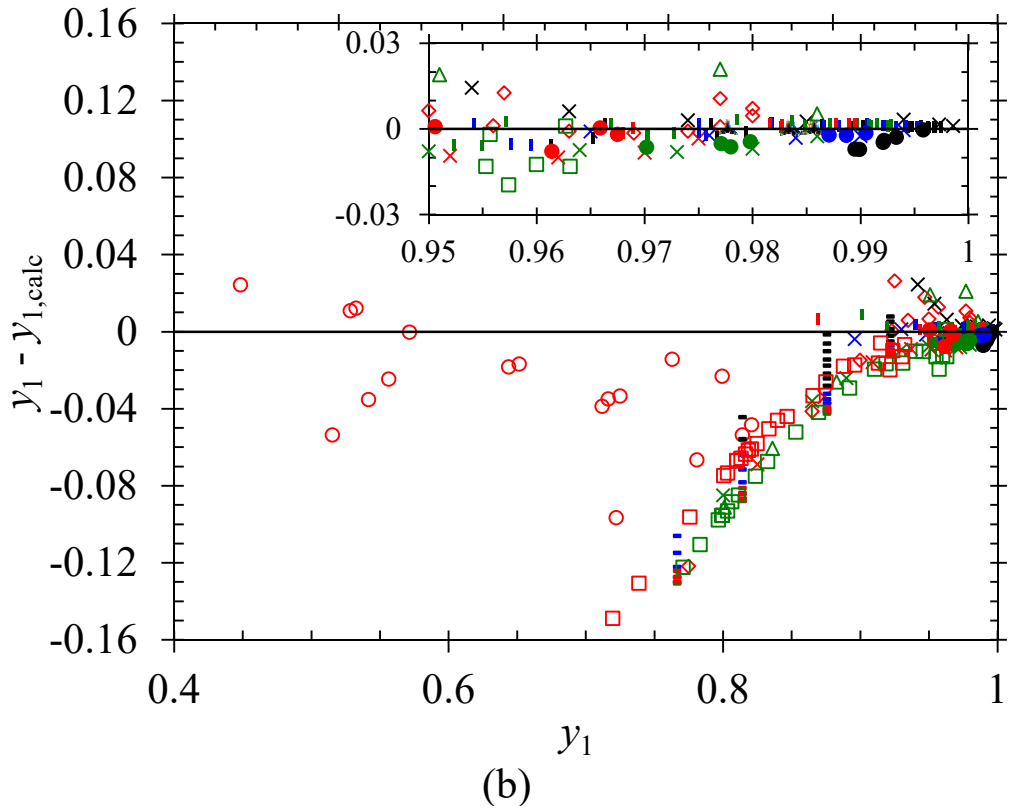

Figure 3. Deviations of the measured mole fractions from those calculated with the PR EOS implemented in Multiflash's PR (advanced) model set [6] (indicated by subscript calc) for methane (1) + benzene (2): (a) deviations of the liquid methane mole fraction x_1 as a function of x_1 and (b) deviations in the vapor methane mole fraction y_1 as a function of y_1; ●, This work (Black: T = 278 K, Blue: T = 303 K, Green: T = 323 K,

Red: T = 348 K); +, Sage et al. [20] (black, T = 311 K; blue, T = 344 K; green, T = 378 K); ◊, Elbishlawi and Spencer [14] (T = 339 K); ×, Stepanova et al. [21] (Black: T = 273 K, Blue: T = 293 K, Green: T = 313 K, Red: T = 333 K); ⅄, Coan and King [12] (T = 323 K); ○, Lin et al. [16] (421 ≤ T/K ≤ 501); ☼, Luks et al. [17] (268 ≤ T/K ≤ 278); Δ, Legret et al. [15] (T = 313 K); ı, Rijkers et al. [2] (Black: 279 ≤ T/K ≤ 285, Blue: 291 ≤ T/K ≤ 297, Green: 303 ≤ T/K ≤ 309, Red: T = 315 K); -, Rijkers et al. [19] (Black: 266 ≤ T/K ≤ 284, Blue: 284 < T/K ≤ 304, Green: 304 < T/K ≤ 325, Red: 325 < T/K ≤ 352); *, Darwish et al. [13] (black, T = 323 K; blue, T = 373 K; green, T = 423 K); □, Marteau et al. [18] (green, T = 323 K; red, T = 373 K).

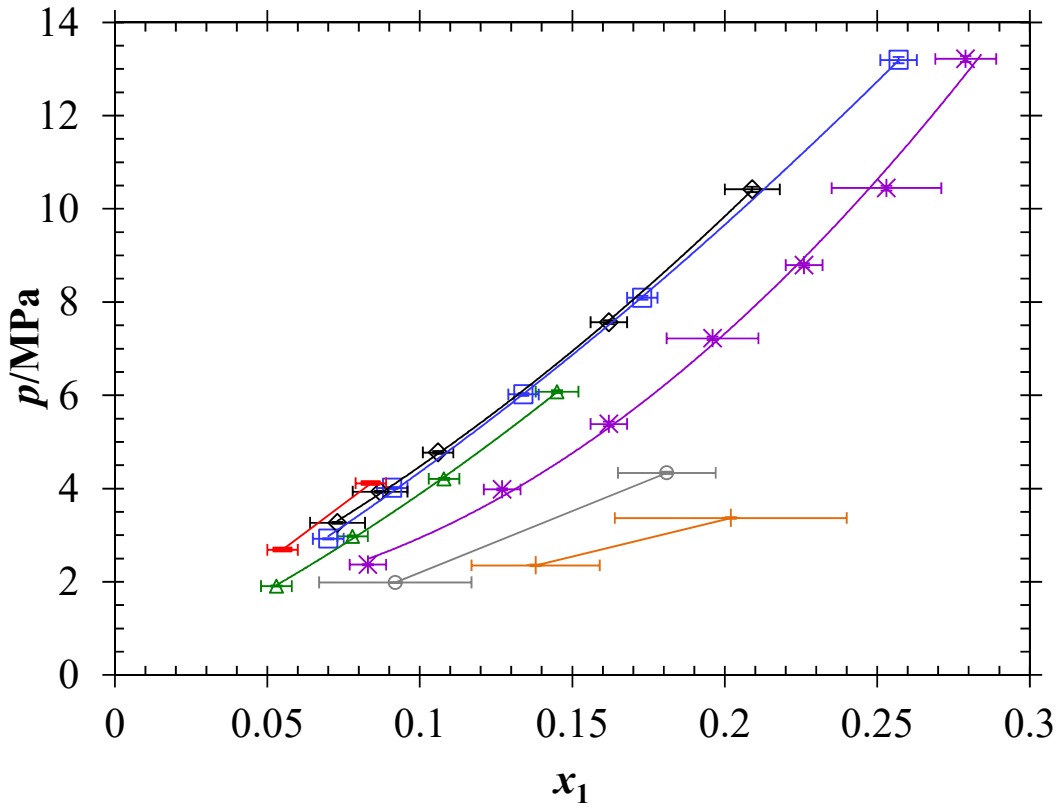

Figure 4. Measured vapor-liquid equilibrium *p, x* data of the methane (1) + methylbenzene (3): +, T = 188.15 K; ○, T = 198.15 K; *, T = 228.15 K; Δ, T = 253.15 K; □, T = 277.65 K; ◊, T= 293.15 K; –, T = 313.15 K. Linear or quadratic trendlines are shown to guide the eye.

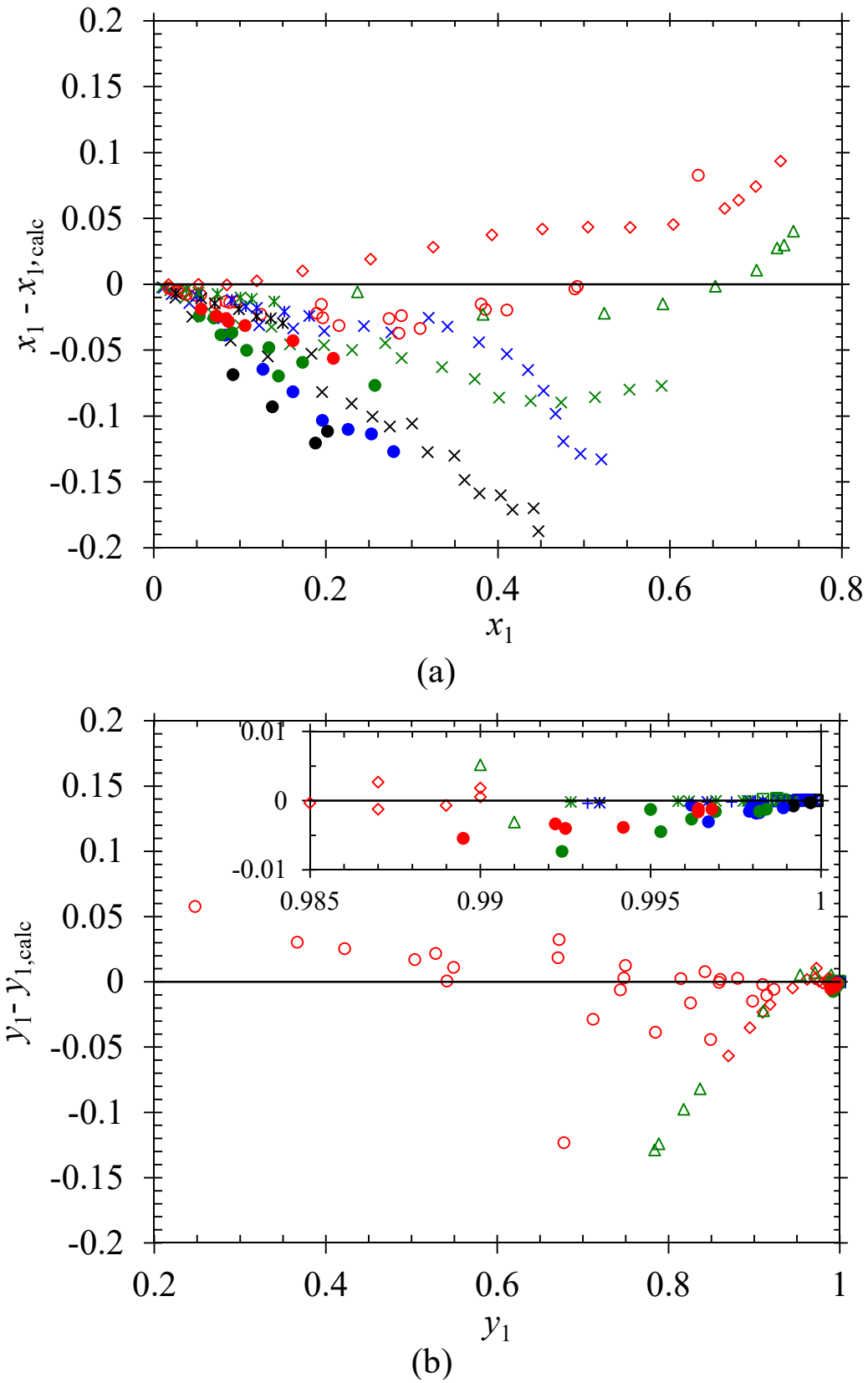

Figure 5. Deviations of the measured mole fractions from those calculated with the PR EOS implemented in Multiflash's PR (advanced) model set [6] (indicated by subscript calc) for methane (1) + methylbenzene (3): (a) deviations of in the liquid mole fraction x_1 as a function of x_1 and (b) deviations in the vapor mole fraction y_1 as a function of y_1; ●, This work (Black: T = (188 and 198) K, Blue: T = 228 K, Green: T = (253 and

278) K, Red: T = (293 and 313) K); ◊, Elbishlawi and Spencer [14] (T = 339 K); +, Hwang et al. [24] (Black: T = 255 K, Blue: T = 266 K, Green: T = 277 K); ×, Lin et al. [1] (Black: T = 233 K, Blue: T = 255 K, Green: T = 277 K); ○, Lin et al. [16] ($422 \leq T/\mathrm{K} \leq 543$); Δ, Legret et al. [15] (T = 313 K); □, Schlichting et al. [25] (Black: T = 243 K, Blue: T = 262 K, Green: T = 283 K); *, Srivatsan et al. [26] (Black: T = 313 K, Blue: T = 339 K, Green: T = 423 K)

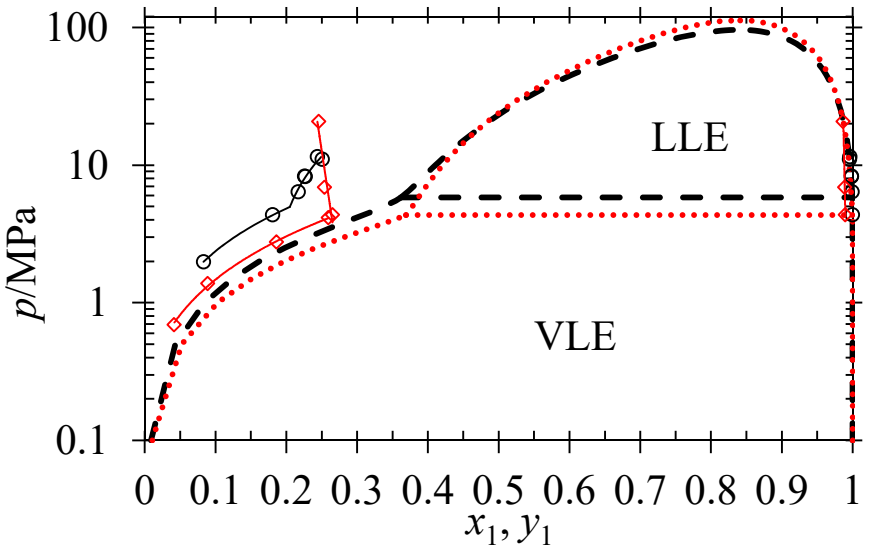
100
10
1
0.1
p/MPa
LLE
VLE
0 0.1 0.2 0.3 0.4 0.5 0.6 0.7 0.8 0.9 1
x1, y1

(a)

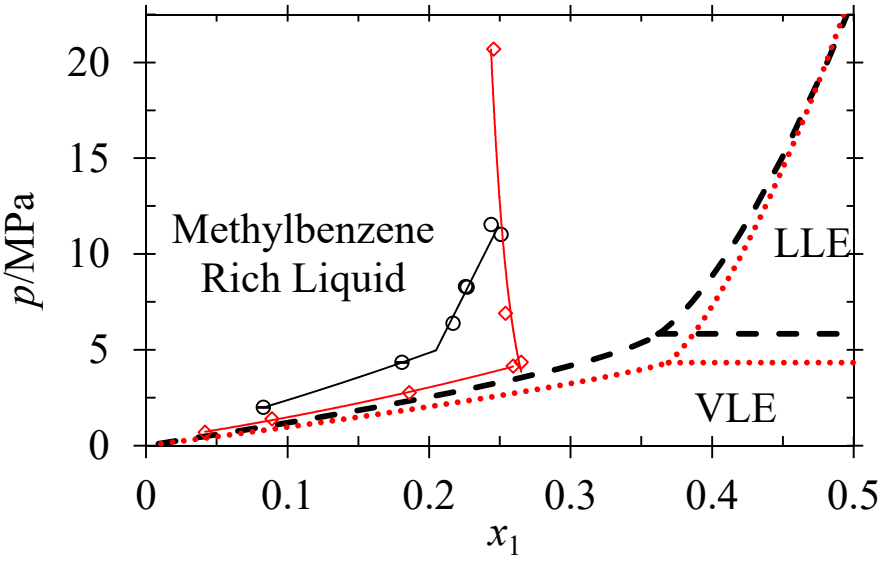
20
15
10
5
0
p/MPa
Methylbenzene
Rich Liquid
LLE
VLE
0 0.1 0.2 0.3 0.4 0.5
x1

(b)

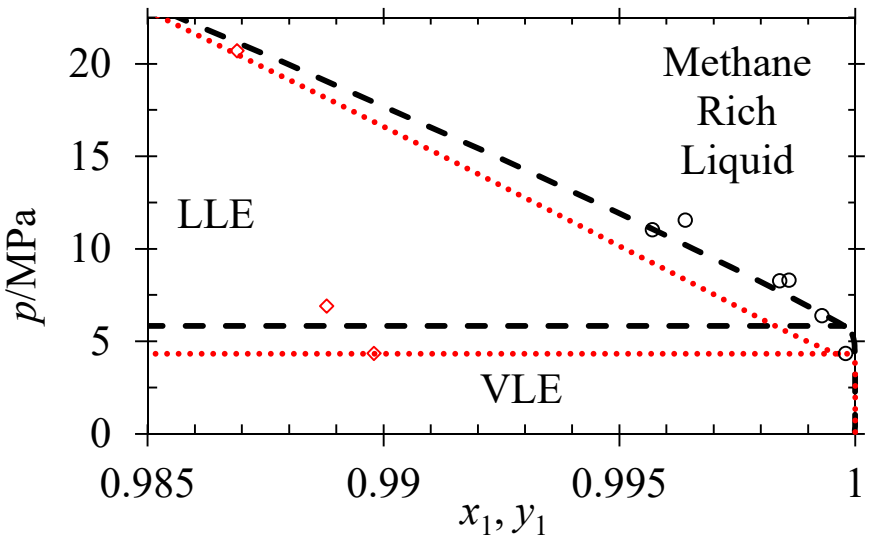
20
15
10
5
0
p/MPa
Methane
Rich
Liquid
LLE
VLE
0.985 0.99 0.995 1
x1, y1

(c)

Figure 6. Vapor liquid equilibrium and liquid-liquid equilibrium in the system methane (1) + methylbenzene (2). ○, This work at $T = 198.15$ K; ◊, Lin et al. [1] at $T = 188.71$ K; ———, PR EOS implemented in Multiflash's PR Advanced model set at $T = 198.15$ K; ••••, PR EOS implemented in Multiflash's PR Advanced model set at at $T = 188.71$ K. (a) The full extent of the VLE and LLE regions calculated using the PR EOS implemented in Multiflash's PR Advanced model set. (b) Close-up of the bubble point lines and methylbenzene-rich LLE lines. (c) Close-up of the dew point lines and methane rich LLE lines: note all the experimental data points shown in part (c), including those of Lin et al. are (V)LLE and should be compared with the sloping methane-rich liquid boundary.

References

[1] Y.-N. Lin, S.-C. Hwang, R. Kobayashi, J. Chem. Eng. Data 23 (1978) 231-234.
[2] M.P.W.M. Rijkers, M. Hathie, C.J. Peters, J. de Swaan Arons, Fluid Phase Equilib. 77 (1992) 343-353.
[3] M.E. Kandil, E.F. May, B.F. Graham, K.N. Marsh, M.A. Trebble, R.D. Trengove, S.H. Huang, J. Chem. Eng. Data 55 (2010) 2725-2731.
[4] M.E. Kandil, M.J. Thoma, T. Syed, J. Guo, B.F. Graham, K.N. Marsh, S.H. Huang, E.F. May, J. Chem. Eng. Data 56 (2011) 4301-4309.
[5] O. Kunz, W. Wagner, J. Chem. Eng. Data 57 (2012) 3032-3091.
[6] Infochem, Multiflash version 4.4, Infochem/KBC Advanced Technologies plc, London, UK, 2014.
[7] Infochem, User Guide for Models and Physical Properties (Multiflash Version 4.4), Infochem/KBC Advanced Technologies plc, London, UK, 2014.
[8] A. Péneloux, E. Rauzy, R. Fréze, Fluid Phase Equilib. 8 (1982) 7-23.
[9] T.J. Hughes, M.E. Kandil, B.F. Graham, E.F. May, International Journal of Greenhouse Gas Control 31 (2014) 121-127.
[10] E.W. Lemmon, M.L. Huber, M.O. McLinden, NIST Standard Reference Database 23: Reference Fluid Thermodynamic and Transport Properties-REFPROP, National Institute of Standards and Technology, Gaithersburg, MD, 2013.
[11] W.A. Dietz, J. Gas. Chromatogr. 5 (1967) 68-71.
[12] C.R. Coan, A.D. King, J. Chromatogr. A 44 (1969) 429-436.
[13] N.A. Darwish, K.A.M. Gasem, R.L. Robinson Jr., J. Chem. Eng. Data 39 (1994) 781-784.
[14] M. Elbishlawi, J.R. Spencer, Ind. Eng. Chem. 43 (1951) 1811-1815.
[15] D. Legret, D. Richon, H. Renon, J. Chem. Eng. Data 27 (1982) 165-169.
[16] H.M. Lin, H.M. Sebastian, J.J. Simnick, K.-C. Chao, J. Chem. Eng. Data 24 (1979) 146-149.
[17] K.D. Luks, J.D. Hottovy, J.P. Kohn, J. Chem. Eng. Data 26 (1981) 402-403.
[18] P. Marteau, J. Obriot, A. Barreau, V. Ruffier-Meray, E. Behar, Fluid Phase Equilib. 129 (1997) 285-305.
[19] M.P.W.M. Rijkers, M. Malais, C.J. Peters, J. de Swaan Arons, Fluid Phase Equilib. 77 (1992) 327-342.
[20] B.H. Sage, D.C. Webster, W.N. Lacey, Ind. Eng. Chem. 28 (1936) 1045-1047.
[21] G.S. Stepanova, Y.I. Vybornova, A.S. Velikovskii, Gazov. Delo 10 (1965) 9-13.
[22] H.H. Anderson, L.D. Shubin, Anal. Chem. 29 (1957) 852-854.
[23] H.L. Chang, R. Kobayashi, J. Chem. Eng. Data 12 (1967) 517-520.
[24] S.-C. Hwang, R. Kobayashi, J. Chem. Eng. Data 22 (1977) 409-410.
[25] H. Schlichting, R. Langhorst, H. Knapp, Fluid Phase Equilib. 84 (1993) 143-163.
[26] S. Srivatsan, W. Gao, K.A.M. Gasem, R.L. Robinson Jr., J. Chem. Eng. Data 43 (1998) 623-625.

Supplementary Material

"Phase Equilibrium Measurements of Methane + Benzene and Methane + Methylbenzene at Temperatures from (188 to 348) K and Pressures to 13 MPa"

Thomas J. Hughes, Mohamed E. Kandil, Brendan F. Graham, Kenneth N. Marsh, Stanley H. Huang, and Eric F. May

Summary

The supporting information contains comparisons of our data to literature data and a discussion of reasons for discrepancies resulting from the review process.

Methane (1) + Benzene (2)

Reviewer comment: *Large deviations of the authors' phase boundary pressures from the literature values are detected for benzene + methane (up to 12 %). The deviations in pressure should be discussed.*

The reviewer's plot for methane (1) + benzene (2) data at T between 276 and 280 K has been reproduced in Figure 1 with uncertainty bars for our data and uncertainties bars for the pressures for Rijkers et al (uncertainties for the mole fractions are not stated) and pressures and mole fractions for the Luks et al from NIST's ThermoData Engine (TDE). Our data are consistent with the literature data within the mole fraction and pressures uncertainties.

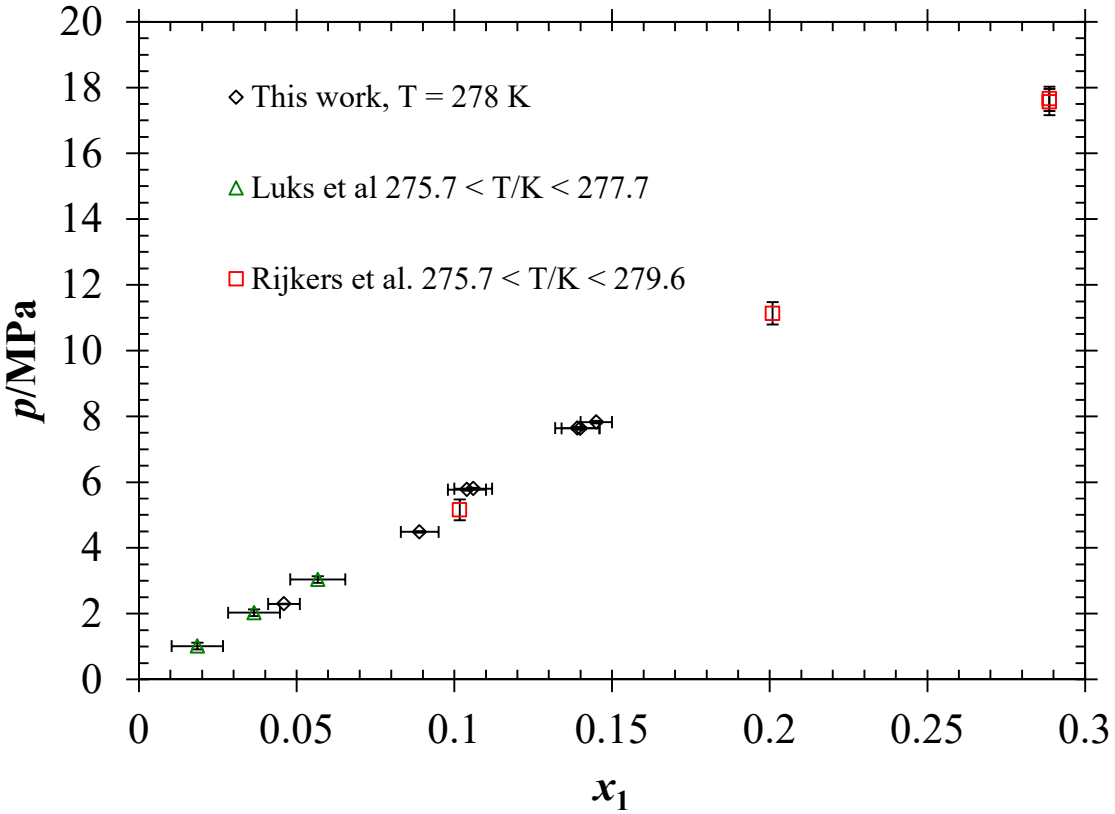

Figure 1. Methane (1) + Benzene (2) bubble point line at about T = 278 K

The reviewer's plot for methane + benzene data at T = 323 K is reproduced in Figure 2 with uncertainty bars for our data and uncertainties bars for the mole fractions for Darwish et al from NIST's TDE. All but the highest pressure point are consistent within the combined uncertainties. We note that the mole fraction

purity of the benzene used by Darwish et al was only 0.978 and the maximum uncertainty in the mole fraction estimated in TDE is perhaps optimistic at 0.0024.

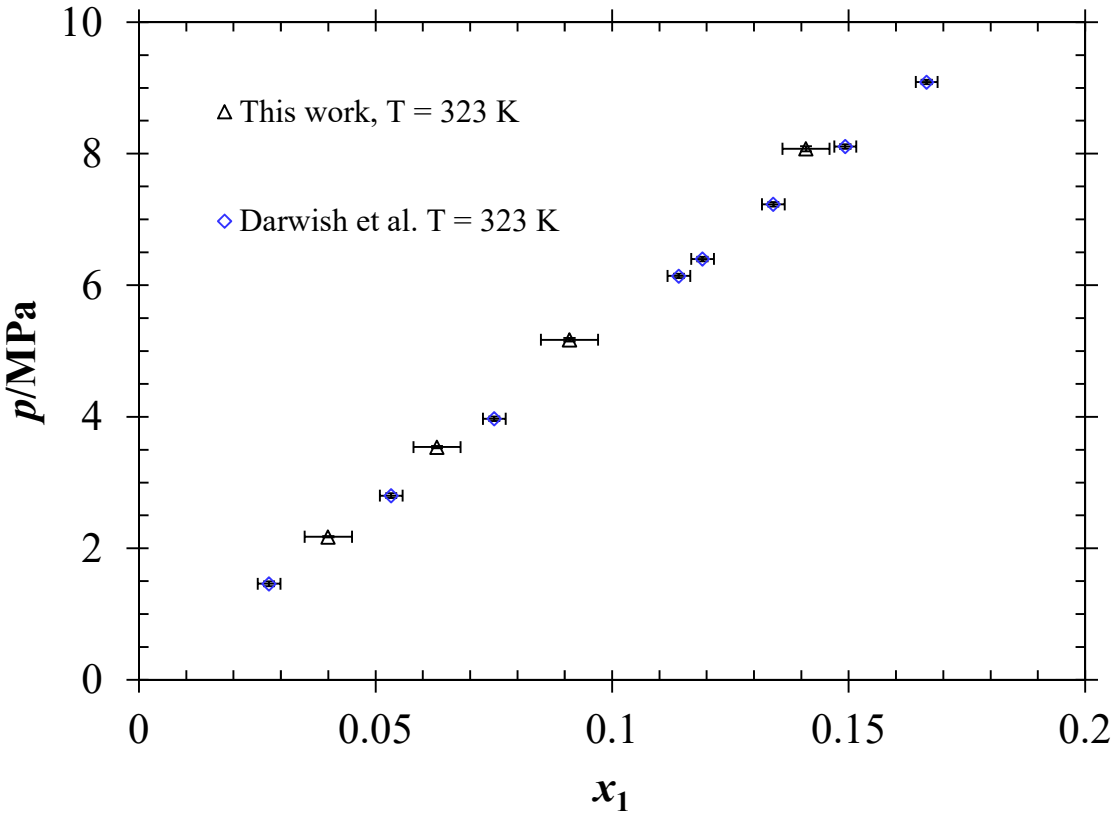

Figure 2. Methane (1) + Benzene (2) bubble point line at about $T = 323$ K

Methane (1) + Methylbenzene (3)

Reviewer comment: *Large deviations of the authors' phase boundary pressures from the literature values are detected for methylbenzene + methane. The deviations in pressure should be discussed.*

The reviewer's plot for methane (1) + methylbenzene (3) data at $T = 278$ K is reproduced in Figure 3 with uncertainty bars for our data and for the mole fractions for Lin et al (1978) from NIST's TDE. We note:

- At low pressures, about $x_1 = 0.07$ to 0.1, our data and Lin et al's data agree within experimental uncertainty.
- Lin et al.'s *p, x* data at $x_1 > 0.1$ then deviate negatively from our data in pressure or positively in methane mole fraction.
- We note a distinctive change in slope of Lin et al's *p,x* data, that occurs at about $x_1 = 0.27$ and $p = 12$ MPa
- NIST's TDE pressure uncertainty for the Lin et al data is always less than 0.2 % of that pressure value
- Lin et al note that pressure uncertainty of their Heise gauges was 0.1 % of full scale. They do not state what the full scales of these gauges were. How TDE estimated these uncertainties in Lin et al (1978) pressure measurements is unclear but it is likely that the pressure uncertainties of some of the points should in fact be higher.
- The use of multiple pressure gauges by Lin et al. appears to have caused shifts and apparent slope changes in their *p,x* data.
- The scatter about the trend of Lin et al's data appears higher than the assigned uncertainties.

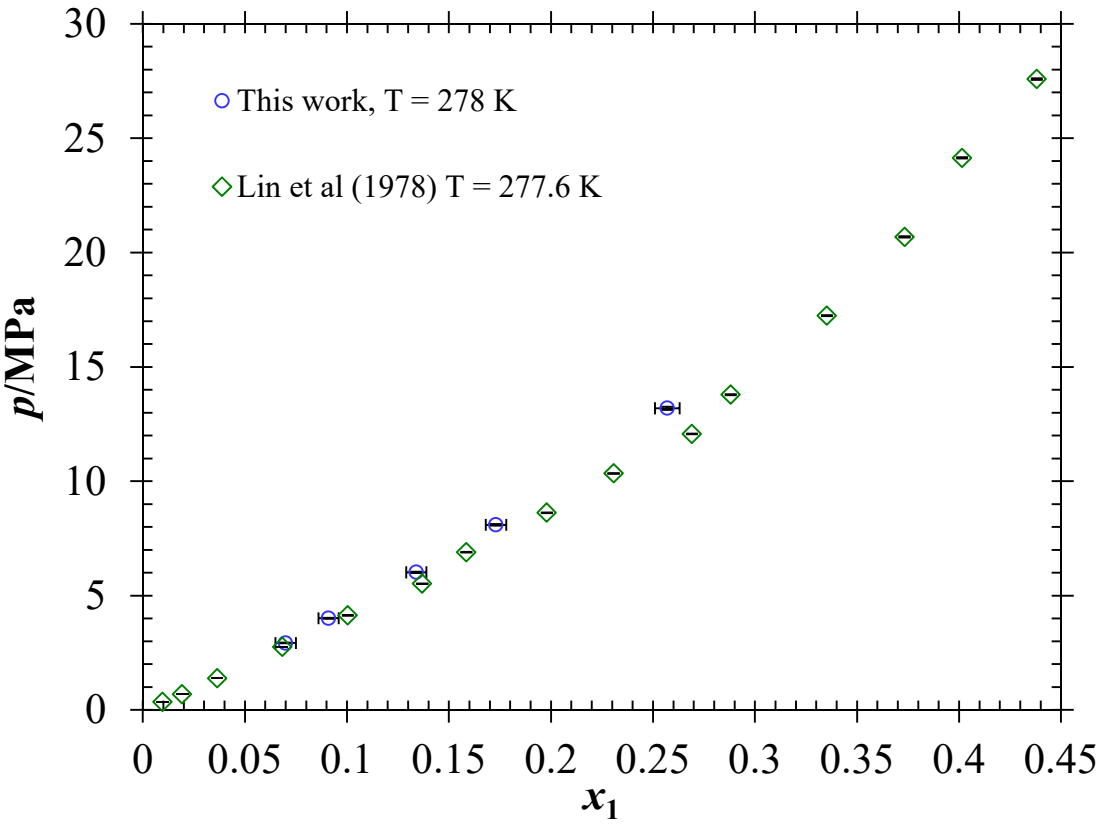

Figure 3. Methane (1) + Methylbenzene (2) bubble point line at about T = 278 K plotted up to p = 30 MPa

The reviewer's plot for methane (1) + methylbenzene (3) data at T = 188 K is reproduced in Figure 4 with uncertainty bars for the mole fraction for our data and uncertainties bars for the pressures for Lin et al (1978) from NIST's ThermoData Engine (TDE). The data are consistent within the mole fraction and pressures uncertainties.

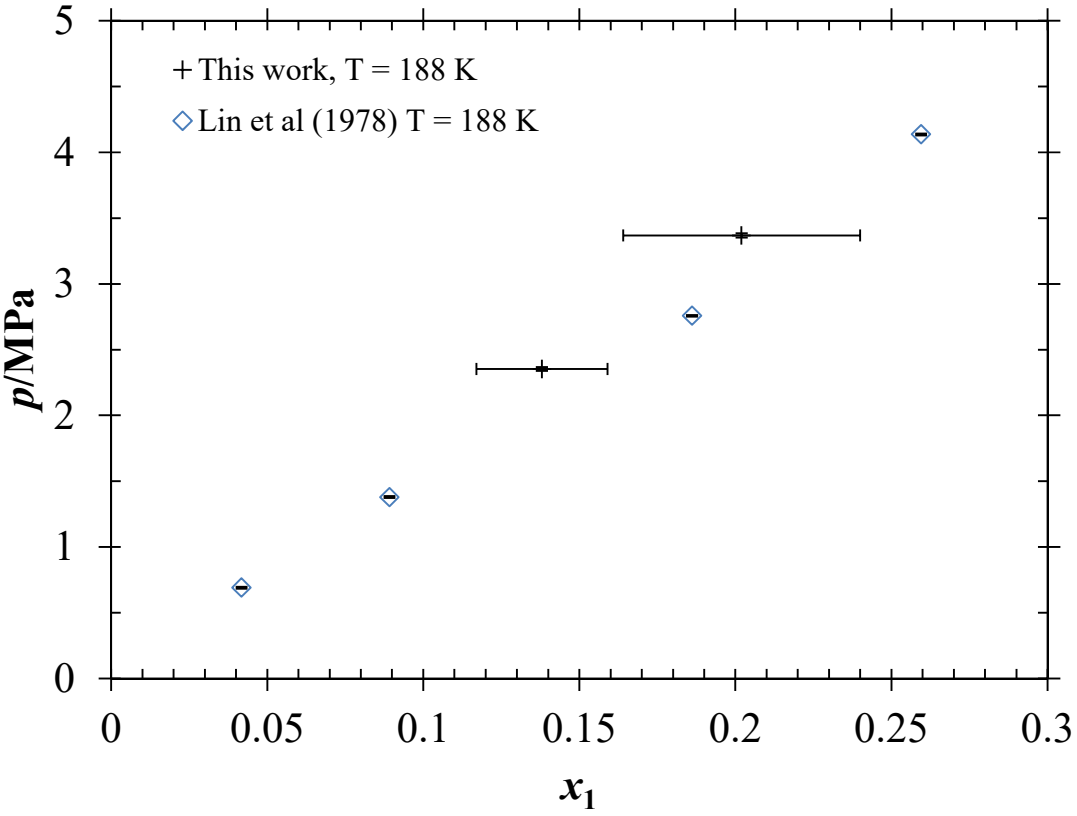

Figure 4. Methane (1) + Methylbenzene (2) bubble point line at about T = 188 K